AIAA JOURNAL
Vol. 47, No. 9, September 2009

Alleviation of Pressure Rise from a High-Speed Train Entering a Tunnel

J. Anthoine*
von Karman Institute for Fluid Dynamics, 1640 Rhode-St-Genèse, Belgium

DOI: 10.2514/1.41109

When traveling through a tunnel, a high-speed train generates pressure waves that propagate back and forth to the portals and affect passenger comfort. Part of the initial compression wave is also radiated at the tunnel's far end, as a micropressure wave, causing environmental nuisance. The strength of this micropressure wave is proportional to the slope of the initial compression wave produced upon train entry, which depends on the geometry of the train and the tunnel entrance and on the blockage ratio. This paper presents a review of the current state of understanding of tunnel entrance aerodynamics for high-speed trains and an experimental assessment of the performance of countermeasures to reduce the slope of the initial pressure rise. A parametric investigation makes use of a scaled-model experimental facility for analyzing the effect of the train velocity and different configurations (conic-shaped train noses, flared portals, vented portals, etc.) on the initial compression wave. It is shown that replacing an abrupt entrance with a progressive one has a beneficial effect on the gradient of the compression wave. A less-costly civil engineering construction consists of distributing ventilation along the tunnel entrance. Among the several distributions tested, the experimentally optimized distribution of the tunnel portal ventilation reduces the slope of the initial pressure rise by a factor of 6.

Nomenclature

l	=	length of the vented region of the tunnel portal
L_{train}	=	train length
M	=	train Mach number
p	=	wave front pressure
p_0	=	static pressure (equal to atmospheric pressure)
R	=	tunnel radius
R_0	=	radius of the holes of the vented portal
t	=	time
U	=	train velocity
x	=	axial position from the tunnel entrance
x_p	=	unsteady pressure probe position from the tunnel entrance
α	=	train nose angle
β	=	blockage ratio
θ	=	azimuthal position of the unsteady pressure probe
ρ	=	air density

Superscript

$*$	=	nondimensional variable

Introduction

HIGH-SPEED trains, such as the French Train à Grande Vitesse and the Japanese Shinkansen, are nowadays offering direct links between city centers at a commercial speed of 360 km/h. When traveling through a tunnel, the high-speed train compresses the stationary air immediately in front of it, causing most of the displaced air to flow over the train and out of the tunnel portal (Fig. 1). The pressure rise propagates into the tunnel at the speed of sound as a compression wave. The overall pressure rise across the front of the compression wave depends critically on the geometry of the train and the tunnel entrance and on the blockage ratio. At the tunnel exit, most of the pressure wave is reflected back as an expansion wave toward the train, which could affect passenger comfort and safety and cause damage to train parts. Part of the initial compression wave is also radiated, as a micropressure wave, from the far end of the tunnel, causing environmental nuisance. The strength of this micropressure wave depends on the slope of the initial compression wave, which might be further steepened due to nonlinear propagation effects in "smooth" tunnels. Although this could cause the micropressure pulse to emerge as an explosive bang, its amplitude is still governed by the initial shape of the pressure rise produced upon train entry. Therefore, countermeasures to reduce the slope of the initial pressure rise will improve passenger comfort on the one hand and limit the environmental nuisance induced by the micropressure wave on the other hand.

The paper serves the dual purpose of reviewing the current state of understanding of tunnel entrance aerodynamics for high-speed trains and also assessing experimentally the performance of countermeasures to alleviate the aforementioned problems. First, the effect of the train's velocity and shape on the slope of the initial pressure rise is quantified through subscale experiments and compared with the literature data. Then, the benefit of modifications to the tunnel entrance via flared and vented portals is assessed. In particular, the motivation of the present work is to obtain an experimentally optimized distribution of the tunnel portal ventilation.

Previous Works

The aerodynamics of high-speed trains has been an active subject, first in Japan and then in Europe, during the last decades [1–3]. A general review of the aerodynamic concerns of a high-speed railway train, including drag, noise and train/tunnel interaction, is provided by Raghunathan et al. [4]. Considerable efforts have been made to study the velocity field and pressure pattern induced by such a train entering a tunnel to design new methods to weaken the pressure variations and the resulting micropressure wave.

Hara [5] developed a comprehensive formula for the overall pressure rise across the compression wave front in a cylindrical tunnel based on the general equations of steady-flow gas dynamics. Pope [6,7] derived a theoretical relation that gives the maximum pressure rise on the tunnel surface, neglecting the preexisting airflow. He used a one-dimensional adiabatic model, employing pressure loss

Presented as Paper 3559 at the 13th AIAA/CEAS Aeroacoustics Conference (28th AIAA Aeroacoustics Conference), Rome, Italy, 21–23 May 2007; received 19 September 2008; revision received 18 May 2009; accepted for publication 4 June 2009.

*Associate Professor, Environmental and Applied Fluid Dynamics Department, Chaussée de Waterloo 72; anthoine@vki.ac.be. Member AIAA.

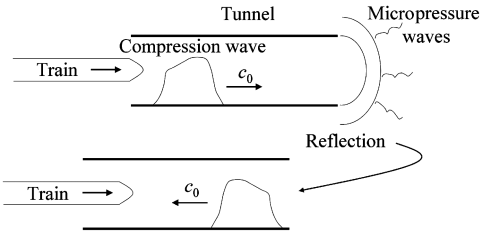

Fig. 1 Schematic of compression wave in front of train head and micropressure wave.

coefficients to account for the effects of viscosity. These coefficients have been measured empirically on a full-scale model. Vardy [8] developed an equivalent formulation but accounted for the pre-existing airflow, which could be quite important. Howe [9–11] studied thoroughly the physical mechanisms that describe the generation of the compression wave at the entrance hood of a tunnel. According to his analysis, acoustic monopole and dipole sources are responsible for the initial pressure rise at the tunnel entrance and for "vortex sound" sources in the airflow displaced by the train out of the tunnel. Sockel [12,13] obtained a rather simple formula providing the amplitude of the first two pressure peaks as a function of the main parameters, such as the Mach number and the blockage ratio, and allowing for skin friction forces on the tunnel and train surfaces. He also compared its predictions to results from viscid flow one-dimensional in space computational fluid dynamics (CFD) calculations. Fujii and Ogawa addressed the problem of pressure wave generation in single- and double-track tunnels by numerical simulations [14] and the influence of the train length on the initial pressure rise [15]. Auvity et al. [16] conducted tunnel pressure and velocity measurements on a 1/140th-scale apparatus, including visualization of the exiting flow from the tunnel entry performed by a laser sheet at the time of the train entrance. Bellenoue et al. [17] performed an experimental investigation based on a reduced-scale test method using low-sound-speed gas mixtures that can reproduce quite well the three-dimensional effects due to the train geometry and its position in the tunnel. They found that the wave front can be considered well established and planar for distances larger than four times the tunnel diameter, allowing three-dimensional models to be advantageously replaced by axially symmetrical models, provided that the longitudinal cross-sectional area profile is the same for both configurations. This also justifies that CFD programs for viscid flow one-dimensional in space give rather reliable results. Bellenoue et al. also proposed the following train nose design procedure: first, determine the cross-sectional profile of a train nose against train/tunnel interactions by means of an axially symmetrical configuration; then, give a three-dimensional shape for drag and stability optimization.

When reaching the far end of the tunnel, the initial pressure rise is partly radiated outside as a micropressure wave. N'Kaoua et al. [18] investigated the influence of the train velocity on the first pressure gradient. They found that for a speed of 42 m/s there is little increase in pressure gradient as the wave propagates along the tunnel. This is in contrast to the situation at 85 m/s, at which there is a very marked increase in pressure gradient over a distance of 4000 m from the entry portal. Starting from the observation that pressure wave propagation in tunnels is mainly a one-dimensional phenomenon, Yoon and Lee [19], Yoon et al. [20], and Baron et al. [21] developed efficient methods capable of capturing the fundamental features of pressure wave propagation within tunnels and predicting the pressure disturbances radiated from tunnel portals. The methods are based on the classical linear acoustic formulation by Kirchhoff, in which the source data are obtained either by the acoustic monopole analysis and the method of characteristics [20], by the solution of the Euler equation [20], or by the solution of the unsteady quasi-one-dimensional equations of gas dynamics [21]. The numerical prediction of the compression wave, the propagation in the tunnel, and the micropressure wave obtained by these different methods show a reasonable agreement with data from both full- and reduced-scale experiments. Other experimental and numerical investigations of the micropressure waves have been performed by Grégoire et al. [22] and Ehrendorfer et al. [23].

To alleviate the worst pressure effects, it is necessary to increase the rise time of the initial pressure wave. The ideal outcome, namely, a linear increase in pressure in the main tunnel, is not quite achievable, but it can be approached quite closely. This can be done either by reducing the amplitude of the wave front or by increasing the time required for it to develop. In practice, the first of these alternatives is rarely achievable, so attention focused primarily on the latter [8]. The most obvious way is to reduce the train speed, knowing that the initial pressure gradient is approximately proportional to U^3, where U is the train velocity. However, this solution is resisted by train operators. The second possibility is to elongate the train nose [24], but the solution is impracticable for existing trains and unsuitable for railways with very few tunnels. Countermeasures on the tunnel entrance are, then, the remaining remedial measure to increase the rise time of the initial pressure wave. One way is to flare the entrance region to get a progressive rate of change of the tunnel area (flared portal). Another is to allow air to escape through holes in the walls of the entrance region (vented portals). As the train moves along that region, the number of holes between it and the main tunnel gradually reduces, and so the proportion of air forced into the main tunnel gradually increases. A recent review of the generation and alleviation of sonic booms from rail tunnels is given by Vardy [8].

Howe [25] has examined analytically the influence of tunnel portal flaring on the initial thickness of the compression wave, assuming the local flow near the tunnel mouth during train entry to be incompressible, which is valid for low train Mach numbers. He found an "optimal" shape of the flared portal corresponding to a constant and overall minimum pressure gradient across the front, so that the pressure in the wave front increases linearly. A formula is proposed for extrapolating these predictions to train Mach numbers as large as 0.4. The predictions are validated by comparison with scale model experiments using axisymmetric trains of various nose profiles projected at 300 km/h along the axis of a cylindrical tunnel fitted with a flared portal [26]. Flared entrances were also previously investigated by Yamamoto [27]. The micropressure wave can also be reduced by adding an expansion chamber at the tunnel exit portal in a manner analogous to a muffler in automotive applications. Aoki et al. [28] investigated the effects of expansion chambers numerically and experimentally and defined optimum dimensions.

An increase of the initial pressure rise can also be obtained by distributing air shafts along the tunnel entrance (vented portals) [29]. The air shafts fragment the wave front as it propagates along the tunnel. At each shaft, the reflection/transmission process for the wave front is such that the amplitude of the leading part of the transmitted wave front is always smaller than that of the incident wave front. Numerical studies focusing on the influence of different kinds of tunnel entrances on the intensity of the compression wave have been performed by Monnoyer and William-Louis [30] and Mok and Yoo [31]. Ozawa et al. [32] proved that side branches with closed ends might be as effective at reducing steepening as shafts with open ends, which is of practical importance because closed branches are feasible in deep tunnels as well as in shallow ones. Howe [33] developed an analytical model to predict the initial pressure rise of a train entering a tunnel for which the entrance is "vented" by perforations. In this model, the tunnel consists of a thin-walled circular cylinder perforated on a finite length of its entrance with an axisymmetric distribution of circular apertures. The initial form of the compression wave is expressed in terms of an equivalent source distribution representing the train and the compact Green's function for sources in the hood [34]. The predictions of the optimal shaft dimensions are, however, too small because the model does not account for separated flows over the train, from the hood portal, and from the peripheries of the windows. This model has been superseded by a much more accurate and rapid numerical prediction method taking into account separated flows through the air shafts and frictional drag on the train and tunnel walls [35]. The numerical method has been extended to include short hoods with lengths as small as just twice the tunnel height and has been validated by experiments at speeds up to 425 km/h [36]. Finally, Howe [37] proposed a genetic algorithm to

yield an optimal design of the tunnel entrance hood, in term of pressure gradient, from among a theoretically unlimited number of possibilities for prescribed values of the train speed and hood dimensions.

Experimental Facility

The experimental study has been carried out with a scale-model test facility (Fig. 2), analogous to those developed by Ozawa [38] and Auvity and Kageyama [39]. The configuration of the tunnel apparatus, designed by Gouriet [40], is axial symmetric, that is, the tunnel has a circular section and the train presents a cylindrical shape with a flat or conical nose.

Train models are either circular or square cylinders (Fig. 3) of 300 or 600 mm long and 40 mm in diameter (the square models present the same cross-sectional area as the circular models). The train tail is flat, whereas different nose angles are considered: $\alpha = 30$, 45, 60, and 90 deg (flat nose). The train is guided inside a 100-mm-inner-diameter and 6-m-long smooth tunnel. The corresponding blockage ratio β, that is, the ratio between the train-model cross section and the tunnel cross section, is equal to 0.14, which is representative of real configurations ranging typically from 0.1 to 0.3 [4]. The scope of the investigation being the characterization of the initial compression wave, the tunnel length is sufficiently large so that the train has passed the end of the tunnel entrance region (including the vented portal) before the reflection of the initial compression wave at the tunnel exit reaches it.

Different shapes of entry portals are considered: simple entry, two entries with flared hoods, and one entry with a parametrized vented hood. The diameter of each flared hood decreases linearly from the hood entrance to the joint with the tunnel with an angle of 12 deg. The two hoods differ by their lengths: 110 and 330 mm. The vented hood is made of a tube with a 100 mm inner diameter (equal to the tunnel diameter) and a length of 500 mm. The tube is perforated by 100 circumferential rows of 19 holes of 3 mm diameter (Fig. 4). The step between the rows along the tunnel axis is 5 mm. The thickness of the tube is reduced to 2 mm to limit the pressure loss through the apertures. The advantage of this perforated entrance is the ease of changing the ventilation distribution by putting tape on part of the multiple holes. Different distributions of openings have been tested to find the experimentally optimized distribution of the tunnel portal ventilation.

The train model is launched thanks to a crossbowlike mechanism (Fig. 5). Because strong acceleration is provided to the scaled model, rolling parts are avoided to drive the model and are replaced by sliding rings made of Teflon® and installed in the nose and in the tail. The model then slides on steel wires passing through the sliding rings and functioning as railways. It passes through the tunnel and is stopped, after the tunnel exit, by a damping mechanism made of rubber foam. A device positioned before the launching mechanism served the purpose of putting the wires in tension to assure the smooth sliding of the train models (Fig. 2).

The crossbowlike launching mechanism permits the train model to reach velocity of up to 42 m/s. Even if this is below the operating velocity of the full-scale high-speed train, the fundamental mechanism of the initial compression wave can still be observed, as shown by Auvity and Kageyama [39]. The increase of the pressure gradient as the wave propagates along the tunnel is underestimated at this low train velocity, as indicated by N'Kaoua et al. [18]. However, this is not the scope of the present study, which focuses on the investigation of the parameters influencing the generation of the

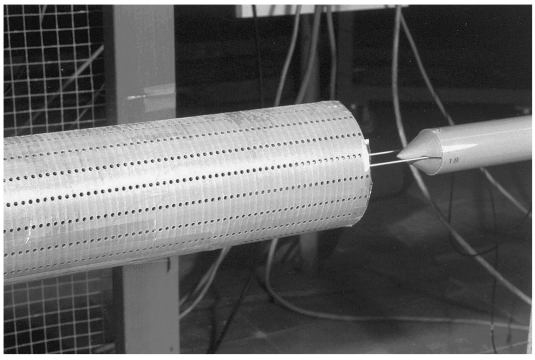

Fig. 4 Vented hood.

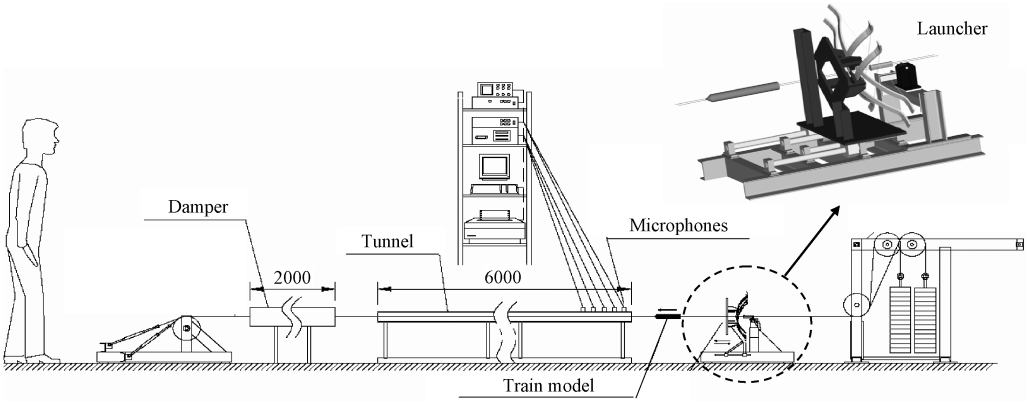

Fig. 2 Experimental facility.

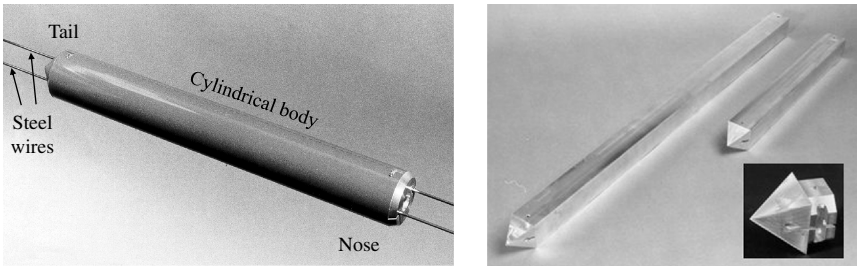

a) Circular train model **b) Square train model**

Fig. 3 Train models.

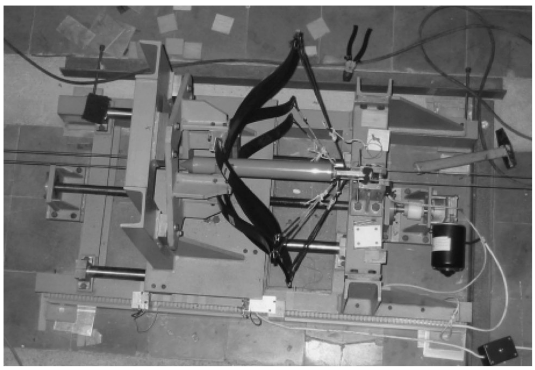

Fig. 5 Crossbowlike launcher.

initial compression wave and on the assessment of the performance of countermeasures to reduce the slope of the initial pressure rise.

The train speed is measured using the photoelectric fiber optic switch WLL160 from Sick Optic Electronic connected to an acquisition card. The detection range of the switch is up to 200 mm, which is larger than the tunnel diameter, and the response time is up to 0.35 ms. When the path between the transmitter and the receiver light guides is obstructed by the train, the switching output is active. The train velocity is achieved by measuring the time interval between the rising and falling steps. The train velocity is controlled at two different points, just upstream of the entry portal and just after the last measurement port at 1180 mm from the entry portal, and is proved to be almost constant during the section of the tunnel along which the pressure and velocity measurements are performed.

The pressure histories are measured with PCB piezoelectric transducers, model 106B50 from PCB Piezotronics, Inc., which are only sensitive to pressure fluctuations. They yield a minimum response time limited only by the mechanical response of the sensing quartz (resonant frequency of 40 kHz) for a pressure range of 34.5 kPa with a resolution of 0.5 Pa. The transducers are flush mounted on the top of the tunnel at 17, 300, 600, 900, and 1180 mm from the tunnel entrance, as shown in Fig. 2.

The pressure signals are amplified by a factor of 50 and filtered at 3 kHz. The train velocity and pressure signals are then acquired by means of an acquisition card at a sampling frequency of 12 kHz. The acquisition process is triggered by the signal of the first photodiode, that is, the acquisition starts with the rising step provided when the train passes in front of this diode. To continue the acquisition process after the crossing of the end part of the train, a reset–set latch is used to maintain the trigger channel at a high level. The measurements have been proved to be repetitive.

Investigation of the Initial Compression Wave

Description of the Pressure Pattern

Figure 6 illustrates the pressure history measured at a stationary point in the tunnel (probe location at 600 mm from tunnel entrance) and evolved by the wave motion. The wave propagation diagram is added to indicate the wave pattern in the tunnel at any time. The major features of the wave motion can be identified in the pressure history plotted in the upper part. Note that the wave diagram is plotted assuming a constant train speed and a constant sound speed (c_0= 340 m/s). In reality, the scaled model decelerates along the tunnel and a time delay appears between the predictions and the measurements for the nose and tail exit waves.

The first pressure increase is given by the arrival of the first compression wave at the probe location (1). This wave starts propagating through the tunnel at the speed of sound as soon as the train head enters the tunnel. The probe flush mounted on the tunnel surface starts to feel an increase of pressure before the kernel of the wave reaches the location of interest. After the passage of the train nose compression wave, the pressure history shows a quite-constant behavior, which depends on the friction effects, before the arrival of the first expansion wave. Afterward, the probe first experiences the passage of the expansion wave generated by the train tail entering the tunnel (2) and then the arrival of the train nose (3). Both these events contribute to a consistent decrease in the pressure. The double step in the pressure decrease is clearly visible. The alignment of the train nose with the probe seems to produce a sharper gradient in the pressure pattern due to the effect of the low-pressure region at the kernel of the separation bubble close to the train nose. Furthermore, the pressure increases (4) due to the passage of the train tail in front of the probe location. Finally, the expansion wave coming from the exit of the tunnel as a reflection of the first compression wave arrives at the location of the probe and this contributes to a decrease in the pressure again (5). The following increase is given by a new compression wave originating from the reflection of the previous rarefaction at the tunnel entrance.

In our facility, the wave packets reflect back and forth without significant attenuation because the tunnel is smooth and the viscous dissipation depends on the tunnel length, which is short in our experiments. In a real tunnel, the pressure wave essentially experiences attenuation and distortion during the propagation processes until it fades out due to viscous friction and heat transfer effects. Figure 7 shows a typical example of the transient pressure evolution at one position close to the entry portal of the tunnel. Still, before the initial pressure rise reaches the tunnel exit for the first time, it might be not attenuated enough or even steepened in the smooth tunnel, so that its reflection could be associated with the radiation of a micropressure wave outside the tunnel. In the following sections, only the initial compression wave measured at one position close to the tunnel entrance will be considered.

Influence of the Train Velocity

The train velocity has an important effect on the generation of the initial compression wave. It is very well known that the first pressure rise and the corresponding pressure gradient are scaling as the square and the cube of the train velocity, respectively. It is then worth using nondimensional variables to drive conclusions valid for all train velocities. The pressure, the time, and the pressure gradient can be adimensionalized as follows:

$$p^* = \frac{p - p_0}{\frac{1}{2}\rho U^2} \tag{1}$$

$$t^* = tU/R \tag{2}$$

$$\left(\frac{\mathrm{d}p}{\mathrm{d}t}\right)^* = \frac{(\frac{\mathrm{d}p}{\mathrm{d}t})R}{\frac{1}{2}\rho U^3} \tag{3}$$

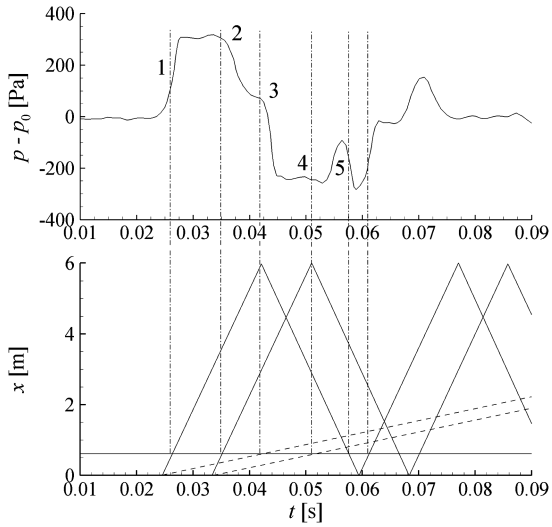

Fig. 6 Correspondence between the unsteady pressure evolution and the wave propagation diagram (solid line: compression and expansion waves; dotted line: position of train nose and tail), $L_{\text{train}} = 300$ mm, circular cross section, $\alpha = 30$ deg, $U = 34$ m/s, and $x_p = 600$ mm.

Fig. 7 Transient pressure evolution measured at 100 m from entry portal for a conventional train traveling in the Patchway tunnel [1] (NP and TP mean, respectively, nose and train passing).

Figure 8 provides the nondimensional evolution of the pressure and pressure gradient measured for different train velocities.

Influence of the Train Nose Shape

To investigate the influence of the nose shape on the pressure pattern, three cone-shaped noses of different angles ($\alpha = 30, 45$, and 60) and a flat nose ($\alpha = 90$ deg) were tested for several vehicle speeds. Figure 9a shows the compression waves measured at 900 mm from the entry portal for $U = 40$ m/s. Figure 9b provides the maximum pressure rise with respect to the nose angle and train velocity. The shape of the compression wave depends on the angle of the cone-shaped nose. Two cases can be distinguished: below 45 deg, the wave front is independent of the nose angle; above this, the maximum pressure increases with the angle. It is interesting to note that the nose shape affects principally the pressure maximum but not the pressure gradient.

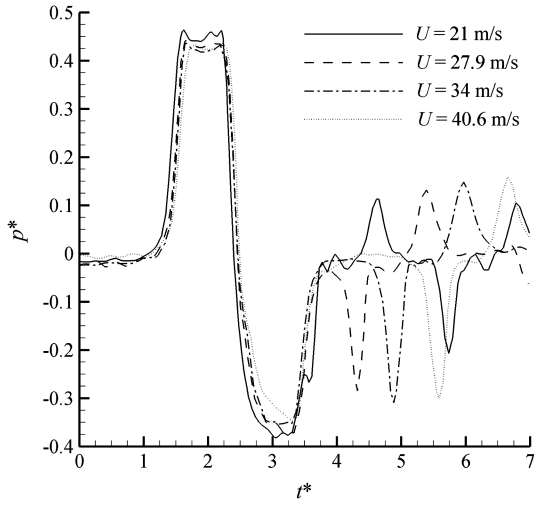

a) Pressure

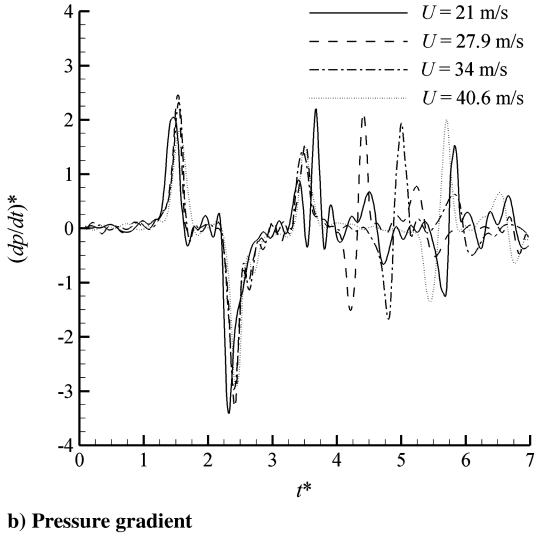

b) Pressure gradient

Fig. 8 Nondimensional evolution of the pressure and pressure gradient, $L_{\text{train}} = 300$ mm, circular cross section, $\alpha = 45$ deg, and $x_p = 300$ mm.

When the train enters the tunnel, the stationary air immediately in front of it is compressed, causing most of the displaced air to flow over the train out of the tunnel. If the nose/train junction presents sharp corners, separated flow regions are developed behind the nose. These regions create a restriction of the section area and an acceleration of the fluid around the train, which is equivalent to an inviscid case with a larger blockage ratio. This corresponds to an increase in the first pressure rise, as found by applying the formulation of Hara [5] (Fig. 9a). When the fluid has passed the separated flow region, it encounters a larger section area and starts to decelerate. This deceleration creates an expansion wave propagating forward at the speed of sound, responsible for the pressure decrease following the first peak in Fig. 9a. The initial larger peak was reported by Hara and Okushi [41] (Fig. 9c), who performed scaled-model experiments for a train velocity of 15 m/s and a blockage ratio of 0.32. They found that the peak disappears if the sharp edge at the transition between the nose and the body is smoothed enough (compare cases c and e) or if the nose angle is small enough even in presence of a sharp corner (compare cases d and e). The results of Figs. 9a and 9b are in good agreement with these observations: the initial larger peak disappears, and the first compression wave becomes independent of the nose angle for nose angles smaller than 45 deg even in the presence of a sharp corner. In the remainder of the paper, only train nose angles of 30 and 45 deg will be considered.

Influence of the Train Cross Section

All the previous tests are obtained for circular cross-sectional models sliding along the axis of an axisymmetric tunnel. Nizamis [42] and Spolaore [43] investigated the influence of asymmetric conditions of the tunnel, of the vertical position of the train within the tunnel, and of the train shape. The effect of the train cross section on the pressure pattern is analyzed by testing a squared cross-sectional train with a 30-deg-angle pyramidal nose and a flat tail. The blockage ratio remains equal to 0.14. The pressure pattern for both the circular and squared models, shown in Fig. 10, are similar. Changing the vertical position of the train in the tunnel or the tunnel cross section by adding a floor on its bottom part while respecting the same blockage ratio proved to have no effect on the pressure pattern [42,43]. This suggests that the pressure waves propagating through the tunnel are essentially plane waves, which are not affected by the shape of the train and tunnel cross section or by the train position in the tunnel. Measurements performed at three different azimuthal positions θ, all of them at 1180 mm from the tunnel entrance, confirm this finding (Fig. 11). This is consistent with the propagation of acoustic waves in long pipe systems.

Influence of the Train Length

The investigation of the train length is performed on squared train models. Two measurements are carried out at the same point along the tunnel (900 mm from the entrance portal) for the same train velocity (32 m/s) and for two identical trains except for their lengths, which were, respectively, equal to 300 and 600 mm (Fig. 12). As expected, the "plateau" region after the first pressure rise is extended for the longer train. This is due to the enlarged time lag between the passing of the first compression wave generated by the train head entering the tunnel and the arrival of the rarefaction wave from the train tail. In theory, for identical velocities and an ambient

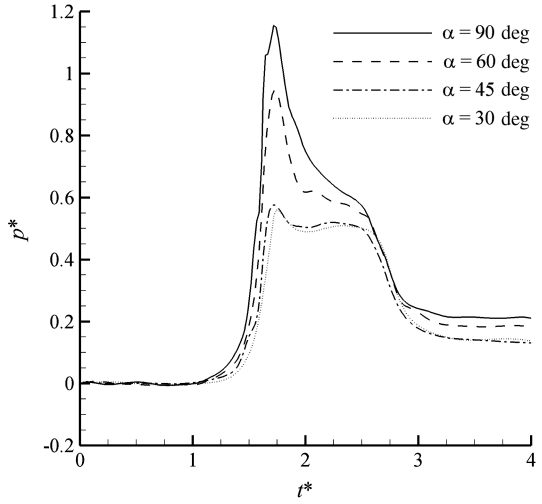

a) Compression waves at U = 40 m/s

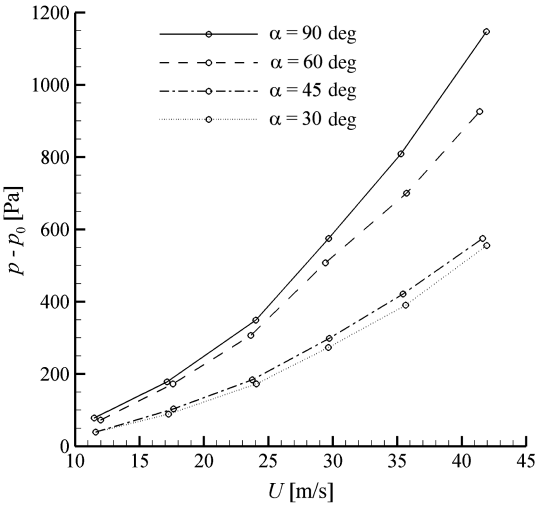

b) Maximum pressure rise

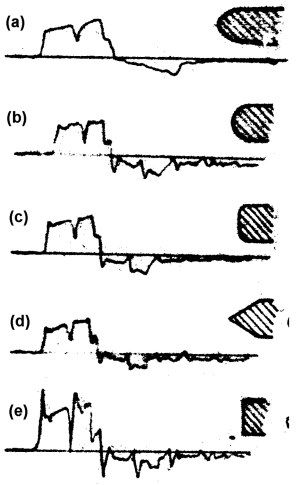

c) Hara and okushi[42]

Fig. 9 Effect of train nose shape on the first pressure rise ($L_{\text{train}} = 300$ mm, circular cross section, and $x_p = 900$ mm) and comparison to experiments from Hara and Okushi [41].

temperature, this time delay should be doubled. Note that, in the case of the long train, the two pressure decreases occurring after the plateau region almost coincide because the effect of the train tail expansion wave and of the alignment of the train head with the microphone nearly superimpose. For the short train, these phenomena are very distinct because the expansion wave reaches the location of measurement before the nose of the model. The rate of pressure rise in the plateau region is slightly bigger for the long train,

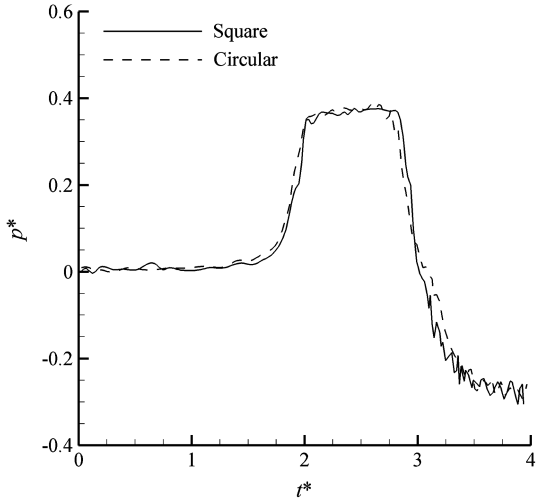

Fig. 10 Effect of train cross section on the first pressure rise, $L_{\text{train}} = 300$ mm, $\alpha = 30$ deg, $U = 38$ m/s, and $x_p = 1180$ mm.

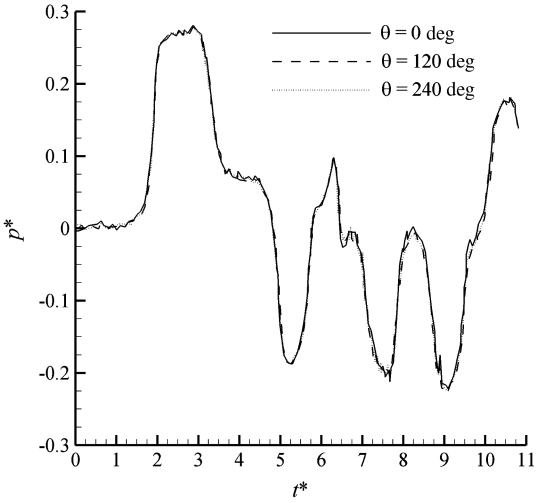

Fig. 11 Axisymmetry of the pressure pattern, $L_{\text{train}} = 300$ mm, square cross section, $\alpha = 30$ deg, $U = 27$ m/s, and $x_p = 1180$ mm.

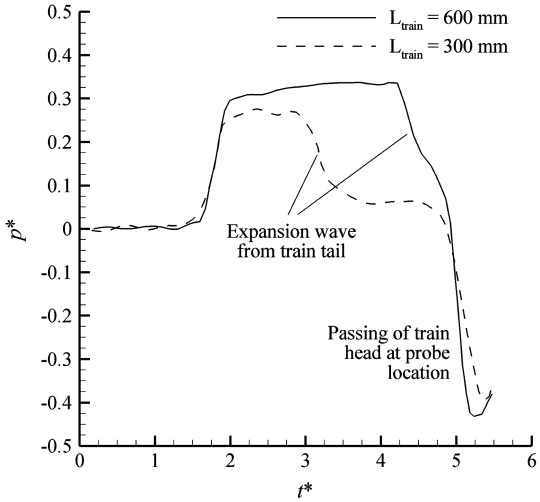

Fig. 12 Influence of train length on the pressure pattern; square cross section, $\alpha = 30$ deg, $U = 32$ m/s, and $x_p = 900$ mm.

suggesting the presence of a thicker boundary layer developing on the train body surface (skin friction effect). Furthermore, the first pressure peak is more intense for the long train. As concluded by Ogawa and Fujii [15], the train length has an influence on the intensity of the pressure peak. The longer the train, the less the length has an influence on the compression wave pressure level. For train lengths similar to those of our experiments, Ogawa and Fujii found an increase in the pressure peak of 23%, which is in good agreement with the difference in maxima of our experimental curves (24%).

Assessment of the Performance of Micropressure Wave Countermeasures

Improving the aerodynamic shape of the train nose or reducing the train velocity could help alleviate the worst pressure effects. However, this requires either modifying the locomotives of the existing trains or accepting a lower efficiency of the train transport system. Another approach to alleviating these pressure effects is modifying the geometry of the tunnel itself. Reducing the blockage ratio by enlarging the tunnel bore would be too expensive and impracticable. A number of techniques involving localized modifications to the tunnel geometry, including flared portal shapes and ventilated entrances, through various forms of air shafts, could be an alternative.

Flared Tunnel Portals

To investigate the influence of the entrance geometry on the primary wave, Ricco [44] tested three configurations. Two of them are flared entrances of 12 deg with different lengths (110 and 330 mm), the third one is an abrupt entrance. No attempt was made during this study to optimize the shape of the flared opening to get a linear pressure rise, as performed by Howe et al. [26]. Figure 13a shows the compression waves measured for a short train with a cone-shaped nose of 45 deg entering the tunnel at 40.6 m/s.

Flared-entry portals prolong the generation of the train entry wave because, for each position of the nose in the convergent, a compression wave appears and propagates forward. Its strength is related to the local blockage ratio. The static pressure starts to increase when the nose enters in the portal, finally reaching the maximum value when the nose leaves the portal at time $t^* = 2.6$ (for the long flare). The multiple compression waves are partly reflected on the convergent walls and propagate backward, reducing the pressure at the train nose. The flaring of the tunnel entrance has also a beneficial effect on the pressure overpeaks, because the flow separation behind the nose does not affect the compression wave for small values of the blockage ratio. The longer the flared portal, the smaller the pressure overpeak.

The results of the present study (Fig. 13a) are in good agreement with the observations of Auvity and Kageyama [39] (Fig. 14), for which the lengths and the angle of the flared entrances are the same as the present tests. Please note that the train length, velocity, and nose angle are not the same for the two investigations, which explains the differences in the curves. The tendencies and the influence of the flared portals remain, however, similar. The use of a convergent entrance for the tunnel decreases the rate of the pressure rise without affecting the maximum pressure significantly (if one does not consider the pressure overpeak). Figure 13b shows the important influence of the flared shape on the pressure gradient. For instance, the long flare reduces the pressure gradient by 75% in comparison with a nonflared entrance. For the short flare, a reduction of 50% is measured. Only the length of the flared portal was modulated, and only a linear shape of the flared opening was considered. An optimization of this shape could have been made to produce a linear pressure rise with the smallest pressure gradient, which is possible to obtain, as indicated by Howe [25]. However, this was not considered because building flared portals for full-scale tunnels is more expensive than realizing vented portals.

Vented Tunnel Portals

Another way to reduce the strength of the micropressure wave is to distribute ventilation along the tunnel entrance. The vented portals are beneficial for two main reasons. First, the initial pressure wave is partially reflected at each opening, so that the amplitude of the transmitted part of the wave is always smaller when traveling along the vented region. Then, the resulting time for the pressure rise is increased. Second, the airflow partially gets out of the tunnel through

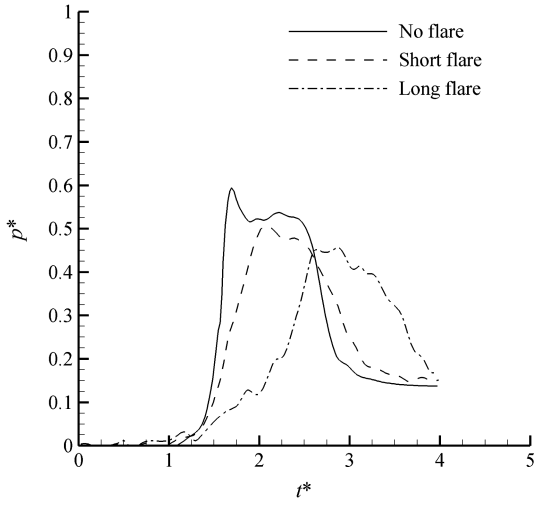

a) Compression waves at $U = 40$ m/s

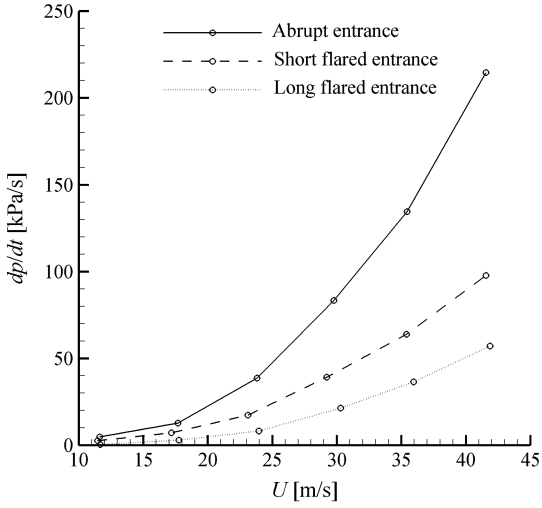

b) Gradient of primary wave

Fig. 13 Influence of different flared-entry portal on the pressure pattern and primary wave, $L_{\text{train}} = 300$ mm, circular cross section, $\alpha = 45$ deg, and $x_p = 300$ mm.

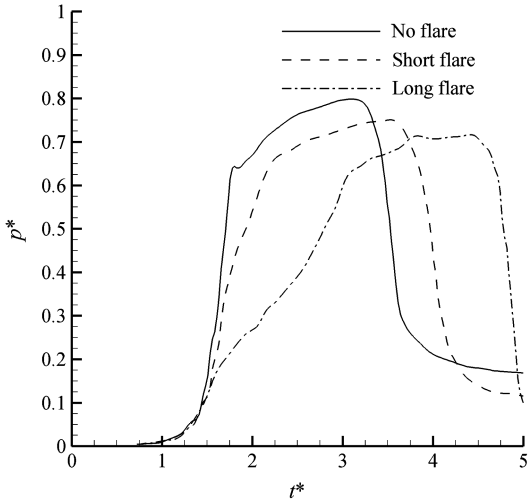

Fig. 14 Data from Auvity and Kageyama [39] on the influence of different flared-entry portals on the pressure pattern and primary wave, $L_{\text{train}} = 600$ mm, circular cross section, $\alpha = 30$ deg, $U = 24.5$ m/s, and $x_p = 200$ mm.

the ventilation in front of the train and enters through the distributed holes located behind the train, with the interesting advantage of reducing the drag.

As indicated in the description of the experimental facility, the vented hood is made of a 500 mm tube perforated by 1900 holes distributed uniformly over all of its surface. The ventilation distribution can then be changed easily by putting tape on part of the multiple holes. Bernard and Jonckheere [45] performed a parametric investigation of the distribution of the ventilation along the tunnel entrance and optimized experimentally this distribution.

Maximum Opening of the Ventilation

A first experiment is made by keeping all 1900 holes open. Figure 15 shows the comparison of the first pressure rise without and with ventilation on the tunnel entrance for a train travelling at 34 m/s (measurement at 600 mm from the tunnel portal, and so 100 mm downstream of the end of the perforated tube). The influence of the distributed holes is not negligible. The pressure rise is longer, which reduces the pressure gradient by a factor of 2. However, the maximum pressure is increased and the pressure rise has been shifted in time. Indeed, the fractional open area being too large, it is transparent to the compression wave generated by the train and delays the first pressure increase.

The solution would be to optimize the ventilation distribution in such a way that the compression starts earlier and the pressure rise time is increased. The optimal situation (indicated with the dotted line in Fig. 15) would be to get a linear increase of the pressure between the time at which the train enters in the tunnel ($t^* = 0.2$) and the time at which it reaches the nonperforated part ($t^* = 1.9$).

Howe Distribution

Howe extended his theory, developed for a profiled train entering a simplified circular tunnel, to different types of tunnel entrances, including the perforated entrance. He derived in 1999 a first distribution law for the tunnel entrance ventilation, aimed at producing a linear pressure rise corresponding to a minimum pressure gradient [33]. The fractional open area $\sigma(x)$ is a smooth function of the axial position along the tunnel (Fig. 16) and is given by

$$\sigma(x) = \frac{\pi R_0}{4R} \frac{1.9(\frac{x}{R})^{9/4}}{(0.4 + (\frac{x}{R})^2)^2} \tag{4}$$

This initial work by Howe has been superseded by a further analysis and calculation of the compression wave generated by a train entering a tunnel with a vented hood [35,36] and by the implementation of a genetic algorithm that applies the previous theories to

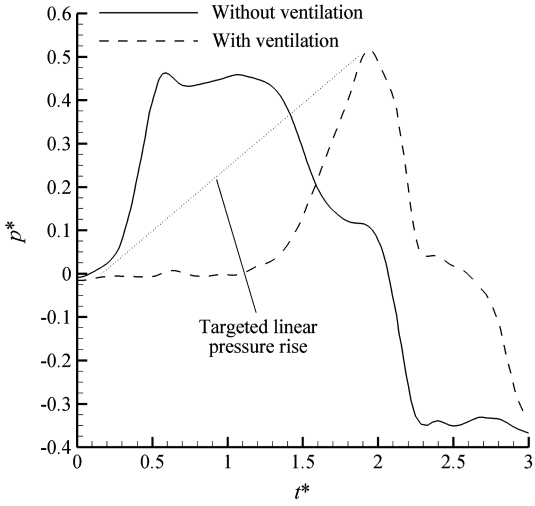

a) Pressure

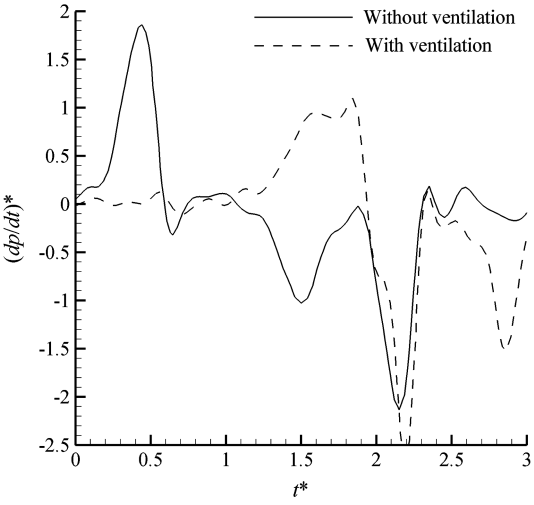

b) Pressure gradient

Fig. 15 Comparison of the pressure pattern without and with ventilation (maximum opening), $L_{\text{train}} = 300$ mm, circular cross section, $\alpha = 30$ deg, $U = 34$ m/s, and $x_p = 600$ mm.

determine an optimal distribution of the tunnel entrance hood [37]. However, only the distribution provided by relation 4 is considered below.

Figure 17 shows the comparison of the first pressure rise with and without tunnel entrance ventilation (Howe distribution, relation 4) for a train entering the tunnel at 34 m/s. The pressure rise is not linear, and the pressure gradient is not constant. However, the parameters of the experiment are very close to the example used by Howe (Table 1). The Mach number is 2 times smaller, but the theory is valid for any Mach number below 0.25. Two possible reasons could explain the deviations: the nose geometry and the pressure losses at the apertures, even though the ratio between the tunnel radius and the aperture radius is respected and care was taken to reduce the thickness of the perforated tube. The obtained results are, however, coherent with the expectation of Howe, who already quoted that the predictions of the optimal shaft dimensions (relation 4) are too small because the model does not account for separated flows.

Search for Increasing the Pressure Rise

The distribution proposed by Howe (relation 4) underestimates the opening surface through which the air could escape. Other ventilation distributions, based on the same fractional open area but multiplied by 3 and 3.5, are considered. The corresponding distributions are shown in Fig. 16, whereas the comparison of the pressure and pressure gradient evolutions are provided in Fig. 17. There is a clear reduction in the maximum pressure gradient when the hole area

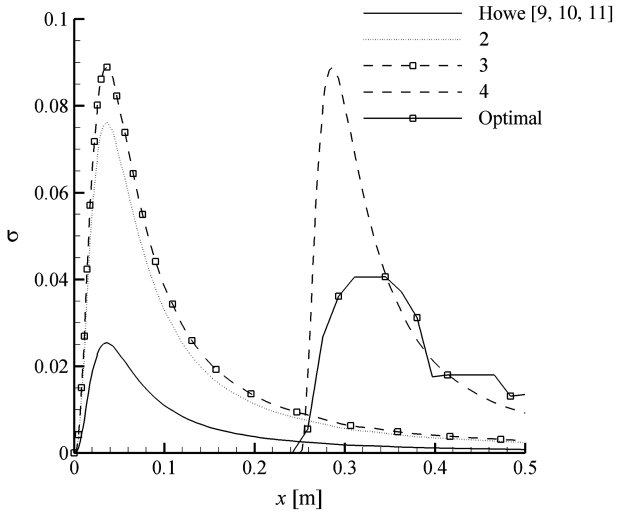

Fig. 16 Ventilation distributions.

is increased. However, the compression wave starts to be generated only when a part of the train is already inside of the tunnel. The pressure rise is longer but shifted, meaning that the opened surface at the entrance of the vented hood is now too large.

Table 1 Comparison of the conditions between Howe [33] and the von Karman Institute experiments

	Howe [33]	von Karman Inst.
M	0.2	0.1
β	0.2	0.16
R/R_0	28	33
l	$10R$	$10R$
α, deg	11.3	30

Search for Shifting the Start of the Pressure Rise

To shift back the pressure rise, the idea is to close the first part of the tunnel portal completely and then to apply the distribution provided by relation 4 (but shifted along x). From groping around and observing the data, the best result was obtained by closing the portal at 0.25 m and applying distribution 3 to the remaining 0.25 m of the tunnel portal. The ventilation opening and the pressure pattern are provided in Figs. 16 and 17, respectively. The compression wave starts to be generated earlier when the train nose is entering the tunnel portal. Even though the pressure gradient is reduced up to $t^* = 1$, it is, however, increasing again for t^* between 1 and 1.5. This peak in the pressure gradient distribution appears when the train nose reaches the reduction of the fractional open area (at $x = 0.3$). All of the previous distributions are then not optimal. Indeed, the pressure rise

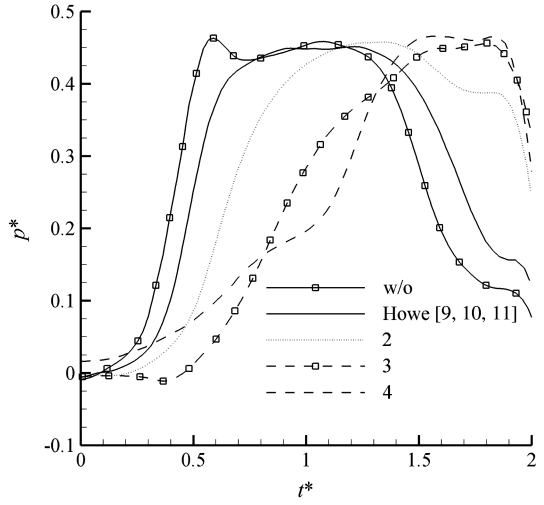

a) Pressure

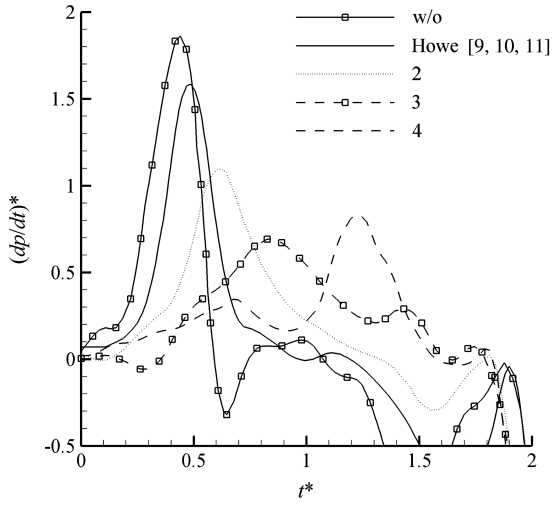

b) Pressure gradient

Fig. 17 Comparison of the pressure pattern for different ventilation distributions, $L_{\text{train}} = 300$ mm, circular cross section, $\alpha = 30$ deg, $U =$ 34 m/s, and $x_p = 600$ mm.

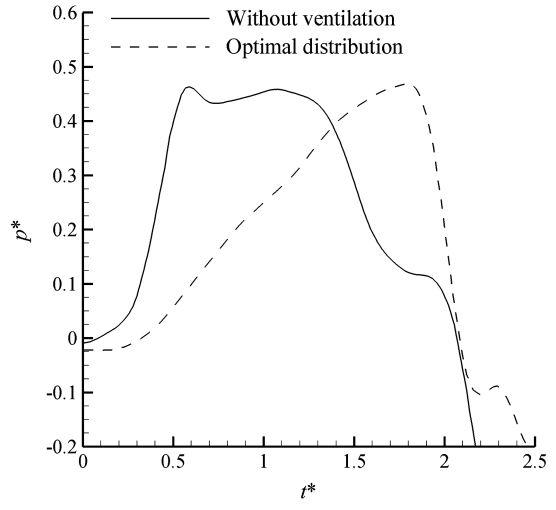

a) Pressure

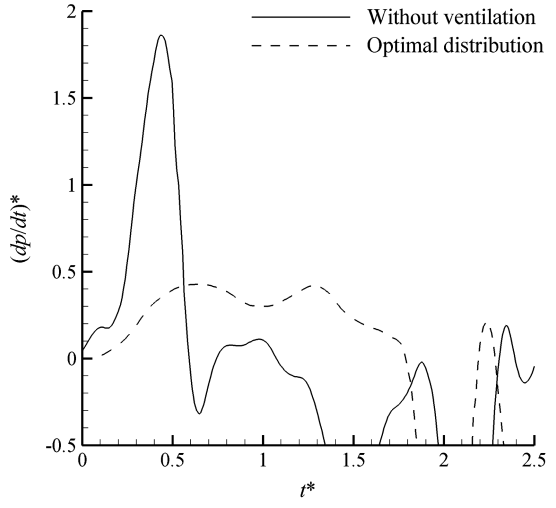

b) Pressure gradient

Fig. 18 Comparison of the pressure pattern when using the optimal distribution of the tunnel entrance ventilation, $L_{\text{train}} = 300$ mm, circular cross section, $\alpha = 30$ deg, $U = 34$ m/s, and $x_p = 600$ mm.

should follow the initial slope of distribution 4 and then continue with the same slope up to the end of the plateau region. This can be achieved by increasing the fractional open area downstream of $x = 0.3$.

Search for an Optimal Ventilation Distribution

From all the aforementioned tests, it seems judicious to close completely the very beginning of the tunnel entrance to force a compression wave as soon as possible and then to increase the fractional open area to release more air in the second part of the vented tunnel. Several ventilation distributions are tested by putting tape on part of the multiple holes to define an optimal configuration. These tests are not presented here, except the last configuration. The optimal distribution of openings in the vented part of the tunnel is given in Fig. 16. This law of distribution is obtained from a step-by-step procedure and is then fully empirical. However, we can observe that the law respects what was expected: a completely closed tunnel at the beginning and then an open area bigger and larger than the Howe distribution in the second part. The pressure rise and gradient are provided in Fig. 18 for a train velocity of 34 m/s. The pressure rise is almost fully linear and starts when the train nose enters the tunnel and finishes when the nose arrives at the end of the vented section. The pressure gradient is reduced by a factor of 6.

The optimized distribution of the tunnel portal ventilation given in Fig. 16 is obtained from scale-model experiments using a porous wall tunnel entrance. Practically, this could be achieved by using a continuous window but with variable height along one lateral side of the tunnel. The continuous window could be structurally strengthened by regularly adding thin vertical profiles. Assuming that the compression waves behave like plane waves, another option to solve the structural problem could be alternating windows on both of the lateral walls of the tunnel in such a way that the combination of these discrete windows is equivalent to a continuous opening respecting the variable fractional open area given in Fig. 16.

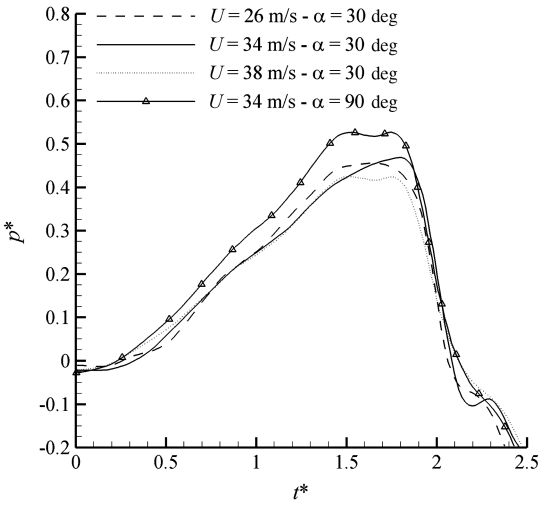

a) Pressure

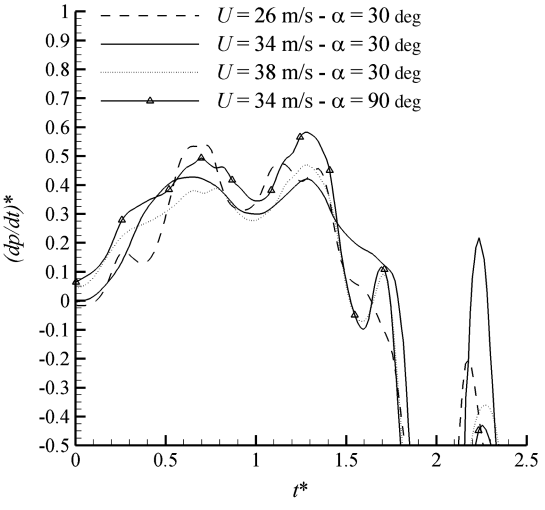

b) Pressure gradient

Fig. 19 Effect of the train nose shape and velocity on the pressure pattern when using the optimal distribution of ventilation, $L_{\text{train}} =$ 300 mm, circular cross section, and $x_p = 600$ mm.

The obvious question now is to see if this distribution is only valid for a train with a nose of 30 deg entering a tunnel at a velocity of 34 m/s. The pressure time histories for different train velocities and nose angles are provided in Fig. 19a. It is clear that the flat nose does not respect the hypothesis of the streamlined nose. It is, however, interesting to compare the results. The velocity has less impact than the nose angle on the pressure rise and then on the pressure gradient. Still, as seen in Fig. 19b, a smaller velocity will provide locally larger pressure gradients. At higher velocities, the pressure rise seems independent from the train velocity. Increasing the nose angle has the negative effect of increasing the pressure gradient all along the pressure rise, but by a limited factor.

Conclusions

A review of the current state of understanding of tunnel entrance aerodynamics for high-speed trains was presented, emphasizing the effect of different parameters, such as the train velocity, length, and nose angle on the initial compression wave. This parametric investigation made use of a scaled-model experimental facility, including a tunnel with different configurations of flared and vented portals. The second part of the paper was devoted to the experimental assessment of the performance of these portals as countermeasures to reduce the slope of the initial pressure rise. This would indeed have a beneficial effect on the strength of the micropressure wave produced at the tunnel far end. Replacing an abrupt entrance with a progressive one reduces the gradient of the compression wave. A less costly civil engineering construction consists of distributing ventilation along the tunnel entrance. Among the several distributions tested, the experimentally optimized distribution of the tunnel portal ventilation reduces the slope of the initial pressure rise by a factor of 6.

Acknowledgments

The author would like to thank the following students of the von Karman Institute who performed some of the measurements presented in this paper: J.B. Gouriet, A. Nizamis, G. Spolaore, F. Bernard, and M. Jonckheere. Particular thanks goes to J.B. Gouriet, who helped in the supervision of the other students during his stay at the von Karman Institute as a research engineer.

References

[1] Gawthorpe, R., "Aerodynamics of Trains in Tunnels," *Railway Engineer International*, Vol. 3, 1978, pp. 41–47.

[2] Schulte-Werning, B., "A Synopsis of Aerodynamic and Aeroacoustic Research for Modern High-Speed Trains," *European Congress on Computational Methods in Applied Sciences and Engineering*, International Center for Numerical Methods in Engineering, Madrid, Sept. 2000, p. 591.

[3] Schetz, J., "Aerodynamics of High-Speed Trains," *Annual Review of Fluid Mechanics*, Vol. 33, 2001, pp. 371–414. doi:10.1146/annurev.fluid.33.1.371

[4] Raghunathan, S., Kim, H., and Setoguchi, T., "Aerodynamics of High Speed Trains," *Progress in Aerospace Sciences*, Vol. 38, 2002, pp. 469–514. doi:10.1016/S0376-0421(02)00029-5

[5] Hara, T., "Aerodynamic Force Acting on High-Speed Train at Tunnel Entrance," *Bulletin of the Japan Society of Mechanical Engineers*, Vol. 4, No. 15, 1961, pp. 547–553.

[6] Pope, C., "Gas Dynamics and Thermodynamics of Unsteady Flow in a Railway Tunnel," Ph.D. Thesis, The Open Univ., Milton Keynes, Buckinghamshire, England, 1986.

[7] Pope, C., "Transient pressures in tunnels: A Formula Predicting the Strength of the Entry Wave Produced by Trains with Streamlined and

Unstreamlined Noses," British Railways Board R&D Division Tech Memo AERO 12, London, 1976.
[8] Vardy, A., "Generation and Alleviation of Sonic Booms from Rail Tunnels," *Proceedings of the Institution of Civil Engineers, Engineering and Computational Mechanics*, Vol. 161, Sept. 2008, pp. 107–119. doi:10.1680/eacm.2008.161.3.107
[9] Howe, M., "Review of the Theory of the Compression Wave Generated When a High-Speed Train Enters a Tunnel," *Proceedings Institution of Mechanical Engineers*, Vol. 213, 1999, pp. 89–104. doi:10.1243/0954409991531056
[10] Howe, M., "On Rayleigh's Computation of the 'End Correction,' with Application to the Compression Wave Generated by a Train Entering a Tunnel," *Journal of Fluid Mechanics*, Vol. 385, 1999, pp. 63–78. doi:10.1017/S0022112098004182
[11] Howe, M., "The Compression Wave Produced by a High-Speed Train Entering a Tunnel," *Proceedings of the Royal Society of London A*, Vol. 454, 1998, pp. 1523–1534. doi:10.1098/rspa.1998.0220
[12] Sockel, H., "Aerodynamic Effects Caused by a Train Entering a Tunnel," *Proceedings in Applied Mathematics and Mechanics*, Vol. 1, No. 1, 2002, pp. 268–269.
[13] Sockel, H., "Formulae for the Calculation of Pressure Effects in Railway Tunnels," *Proceedings of the 11th International Symposium on the Aerodynamics and Ventilation of Vehicle Tunnels*, BHR Group, Cranfield, England, U.K., July 2003, pp. 581–595.
[14] Fujii, K., and Ogawa, T., "Aerodynamics of High-Speed Trains Passing by Each Other," *Computers and Fluids*, Vol. 24, 1995, pp. 897–908. doi:10.1016/0045-7930(95)00024-7
[15] Ogawa, T., and Fujii, K., "Numerical Investigation of Three-Dimensional Compressible Flows Induced by a Train Moving into a Tunnel," *Computers and Fluids*, Vol. 26, 1997, pp. 565–585. doi:10.1016/S0045-7930(97)00008-X
[16] Auvity, B., Bellenoue, M., and Kageyama, T., "Experimental Study of the Unsteady Aerodynamic Field Outside a Tunnel During a Train Entry," *Experiments in Fluids*, Vol. 30, 2001, pp. 221–228. doi:10.1007/s003480000159
[17] Bellenoue, M., Moriniere, V., and Kageyama, T., "Experimental 3-D Simulation of the Compression Wave, Due to Train-Tunnel Entry," *Journal of Fluids and Structures*, Vol. 16, No. 5, 2002, pp. 581–595. doi:10.1006/jfls.2002.0444
[18] N'Kaoua, J., Pope, C., and Henson, D., "A Parametric Study into the Factors Affecting the Development and Alleviation of Micro-Pressure Waves in Railway Tunnels," *Proceedings of the 12th International Symposium on the Aerodynamics and Ventilation of Vehicle Tunnels*, BHR Group, Cranfield, England, U.K., 2006, pp. 789–803.
[19] Yoon, T., and Lee, S., "Efficient Prediction Methods for the Micro-Pressure Wave from a High-Speed Train Entering a Tunnel Using the Kirchhoff Formulation," *Journal of the Acoustical Society of America*, Vol. 110, No. 5, 2001, pp. 2379–2389. doi:10.1121/1.1409374
[20] Yoon, T., Lee, S., Hwang, J., and Lee, D., "Prediction and Validation of the Sonic Boom by a High-Speed Train Entering a Tunnel," *Journal of Sound and Vibration*, Vol. 247, No. 2, 2001, pp. 195–211. doi:10.1006/jsvi.2000.3482
[21] Baron, A., Molteni, P., and Vigevano, L., "High-Speed Trains: Prediction of Micro-Pressure Wave Radiation from Tunnel Portals," *Journal of Sound and Vibration*, Vol. 296, No. 1–2, 2006, pp. 59–72. doi:10.1016/j.jsv.2006.01.067
[22] Grégoire, R., Réty, J., Masbernat, F., Morinière, V., Bellenoue, M., and Kageyama, T., "Experimental Study (scale 1/70th) and Numerical Simulations of the Generation of Pressure Waves and Micro-Pressure Waves Due to Highspeed Train-Tunnel Entry," *Proceedings of the 9th International Symposium on the Aerodynamics and Ventilation of Vehicle Tunnels*, BHR Group, Cranfield, England, U.K., 1997, pp. 877–903.
[23] Ehrendorfer, K., Reiterer, M., and Sockel, H., "Numerical Investigation of the Micro-Pressure Waves," *Proceedings of the TRANSAERO—A European Initiative on Transient Aerodynamics for Railway System Optimisation, Notes on Numerical Fluid Mechanics and Multidisciplinary Design*, Vol. 79, Springer, New York, 2002, pp. 290–301, 321–341.
[24] Maeda, T., Matsumura, T., Iida, M., Nakatani, K., and Uchida, K., "Effect of Shape of Train Nose on Compression Wave Generated by Train Entering Tunnel," *Proceedings of the International Conference on Speedup Technology for Railway and Maglev Vehicles*, Vol. 2, DSME, Japan, 1993, pp. 315–319.
[25] Howe, M., "On the Compression Wave Generated When a High-Speed Train Enters a Tunnel with a Flared Portal," *Journal of Fluids and Structures*, Vol. 13, No. 4, 1999, pp. 481–498. doi:10.1006/jfls.1999.0217
[26] Howe, M., Iida, M., Fukuda, T., and Maeda, T., "Theoretical and Experimental Investigation of the Compression Wave Generated by a Train Entering a Tunnel with a Flared Portal," *Journal of Fluid Mechanics*, Vol. 425, 2000, pp. 111–132. doi:10.1017/S0022112000002093
[27] Yamamoto, A., "On the Gradual Pressure Rise by a Flared Tunnel Entrance," *Quarterly Report of RTRI*, Vol. 6, No. 4, 1965, pp. 50–52.
[28] Aoki, T., Vardy, A., and Brown, J., "Passive Alleviation of Micro-Pressure Waves from Tunnel Portals," *Journal of Sound and Vibration*, Vol. 220, No. 5, 1999, pp. 921–940. doi:10.1006/jsvi.1998.2006
[29] Vardy, A., "Ventilated Approach Regions for Railway Tunnels," *Transportation Engineering Journal of the American Society Of Civil Engineers*, Vol. 101, No. 4, 1975, pp. 609–619.
[30] Monnoyer, F., and William-Louis, M., "Application of CFD to High-Speed Trains Aerodynamics," *Computational Methods in Applied Sciences '96*, Wiley, 1996, pp. 153–159.
[31] Mok, J., and Yoo, J., "Numerical Study on High-Speed Train and Tunnel Hood Interaction," *Journal of Wind Engineering and Industrial Aerodynamics*, Vol. 89, 2001, pp. 17–29. doi:10.1016/S0167-6105(00)00021-0
[32] Ozawa, S., Fukuda, T., Iida, M., Murata, K., and Maeda, T., "Countermeasures for Reducing Micro-Pressure Wave at the Stage of Propagation of the Compression Wave Through a Tunnel," *Proceedings of the 11th International Symposium on the Aerodynamics and Ventilation of Vehicle Tunnels*, BHR Group, Cranfield, England, U.K., July 2003, pp. 389–402.
[33] Howe, M., "Prolongation of the Rise Time of the Compression Wave Generated by a High-Speed Train Entering a Tunnel," *Proceedings of the Royal Society of London*, Vol. 455, 1999, pp. 863–878.
[34] Howe, M., "On the Design of a Tunnel-Entrance Hood with Multiple Windows," *Journal of Sound and Vibration*, Vol. 273, No. 1–2, 2004, pp. 233–248. doi:10.1016/S0022-460X(03)00498-X
[35] Howe, M., Iida, M., Maeda, T., and Sakuma, Y., "Rapid Calculation of the Compression Wave Generated by a Train Entering a Tunnel with a Vented Hood," *Journal of Sound and Vibration*, Vol. 297, No. 1–2, 2006, pp. 267–292. doi:10.1016/j.jsv.2006.03.039
[36] Howe, M., Winslow, A., Iida, M., and Fukuda, T., "Rapid Calculation of the Compression Wave Generated by a Train Entering a Tunnel with a Vented Hood: Short Hoods," *Journal of Sound and Vibration*, Vol. 311, No. 1–2, 2008, pp. 254–268. doi:10.1016/j.jsv.2007.09.012
[37] Howe, M., "The Genetically Optimized Tunnel-Entrance Hood," *Journal of Fluids and Structures*, Vol. 23, No. 8, 2007, pp. 1231–1250. doi:10.1016/j.jfluidstructs.2007.06.005
[38] Ozawa, S., "Studies of Micro-Pressure Wave Radiated from a Tunnel Exit," Railway Technical Research, Rept. 1121, 1979 (in Japanese).
[39] Auvity, B., and Kageyama, T., "Etude Expérimentale and Numérique de l'Onde de Compression Générée par l'Entrée d'un Train dans un Tunnel," *Comptes Rendus de l'Académie des Sciences*, Vol. 323, No. Série IIb, 1996, pp. 87–94.
[40] Gouriet, J., "Aerodynamics of Trains," von Karman Institute, Rept. 1999-16, 1999.
[41] Hara, T., and Okushi, J., "Model Tests on Aerodynamical Phenomena of High Speed Train Entering a Tunnel," *Quarterly Report of the Railway Technical Research Institute*, Vol. 4, 1962.
[42] Nizamis, A., "Experimental Investigation of the Aerodynamics of a Train Entering a Confined Area," von Karman Institute, Rept. 2000-14, 2000.
[43] Spolaore, G., "Aerodynamics of a High-Speed Train Entering a Gallery with Airshafts," von Karman Institute, Rept. 2001-28, 2001.
[44] Ricco, P., "Investigation of Pressure Waves Generated by a High-Speed Train Entering a Gallery," von Karman Institute, Rept. 2001-24, 2001.
[45] Bernard, F., and Jonckheere, M., "Etude des Ondes de Pression Générées par un Train à Grande Vitesse Entrant dans un Tunnel," Master's Thesis, Univ. Catholique de Louvain-la-Neuve, Belgium, 2002.

C. Bailly
Associate Editor